



Research Article

ISSN : 0975-7384  
CODEN(USA) : JCPRC5

## Effect of *Lavandula stoechas* oil on welded material corrosion in 5.5M H<sub>3</sub>PO<sub>4</sub> solution

Abdellah Laqhaili<sup>\*1</sup>, Abdelhak Hakiki<sup>1</sup>, Mahjouba Mossaddak<sup>1</sup>, Maria Boudalia<sup>2</sup>, Abdelkadir Bellaouchou<sup>2</sup>, Abdellah Guenbour<sup>2</sup>, Mohammed El Morhit<sup>3</sup> and Belkheir Hammouti<sup>4,5</sup>

<sup>1</sup>Laboratory of Natural Substances and Thermolysis Lightning, Department of Chemistry, Mohammed V University, Faculty of Science, Agdal, Rabat, Morocco

<sup>2</sup>Laboratory of Materials, Nanotechnology and Environment, Faculty of Science, University of Mohamed-V- Agdal- Rabat, Morocco

<sup>3</sup>Biology Department, Faculty of Science, University of Mohamed V Agdal, Scientific Institute, Rabat, Morocco

<sup>4</sup>LCAE-URAC18, Faculté des Sciences, Université Mohammed Premier, Oujda, Morocco

<sup>5</sup>Petrochemical Research Chair, Chemistry Department, College of Science, King Saud University, Riyadh, Saudi Arabia

### ABSTRACT

Due to problems of resistance to corrosion, the activity of essential oils has now experienced a great revival. Study of the essential oil of the plant *Lavandula stoechas* was studied in 2012 in Doukkala area with relation to the agricultural. The results show that the level of the oil extracted there is a majority molecule (*L*-fenchone) with a percentage of 26 via CPG coupled with MS. The influence of phosphate of organic oil of leaves of *Lavandula stoechas* [L] on the corrosion inhibition of welded material in phosphoric acid solution was studied using the weight-loss method. The electrochemical performance of the inhibitor was also investigated through potentiodynamic polarization. The inhibition efficiency of inhibitor increases with concentration to attain 89 % at 1.2 g.L<sup>-1</sup> of [L] in the phosphoric acid (40 wt. %) or 5.5M H<sub>3</sub>PO<sub>4</sub> with the addition of chemical impurities (4 wt. % of H<sub>2</sub>SO<sub>4</sub> and 0.04 wt. % of chloride ions used as KCl). Polarization studies show that [L] is an anodic-type inhibitor and acts the anodic reactions. The inhibition efficiency of [L] is temperature-dependent in the range 298 - 363 K, the associated activation energy has been determined. [L] Adsorbs on the welded material surface according to a Langmuir isotherm adsorption model.

**Key words:** inhibitor, corrosion, Polarization, CPG, *Lavandula stoechas*, medicinal aromatic plant.

### INTRODUCTION

Industrial phosphoric acid solutions are chemically complex and their analysis change from one plant to another, depending on the quality of phosphate rocks and the process used in their manufacture. Phosphoric acid usually is produced by digestion of phosphate ores with sulfuric acid (H<sub>2</sub>SO<sub>4</sub>) by wet-process phosphoric acid (WPA). This process that is favored by the presence of chemical impurities factors such as abrasion. Corrosion problems occurring in WPA plants have been examined extensively [1,9].

Phosphoric acid in pure state it is not very corrosive compared with other acids. However, phosphoric acid causes corrosion problems during its extraction manufacturing process due to the presence of impurities such as chlorides and sulphates. Moreover, temperature aggravates the corrosion process [7,10,11]. As a consequence, Materials used in this environment must have a good chemical and mechanical resistance. These two characteristics are not always easy to obtain and we have to make compromises between these properties [12]. In this sense, austenitic stainless

steels are a good choice to be used in phosphoric media. In this work a highly alloyed austenitic stainless steel (UB6) was used as a welded material obtained by TIG (Tungsten Inert Gas) process.

However, the welded stainless steel is appropriate owing to their low carbon content. Welding introduces metallurgical changes and residual stresses in materials, diminishing their corrosion resistance [13,14]. The welding process alters the microstructure of the materials, causing local variations in the composition and structure of the material [13].

The use of inhibitors is one of the best options of protecting metals against corrosion [15-22]. Green corrosion inhibitors are biodegradable and do not contain heavy metals or other toxic compounds. The successful uses of naturally occurring substances to inhibit the corrosion of metals in acidic and alkaline environment have been reported by some research groups [23,24]. The encouraging results obtained by *Lavandula* [25-27] incited us to test its inhibiting effect on the welded material in the phosphoric acid (40 wt. %) or 5.5M H<sub>3</sub>PO<sub>4</sub> with the addition of chemical impurities (4 wt. % of H<sub>2</sub>SO<sub>4</sub> and 0.04 wt. % of chloride ions used as KCl). The acidity level of 5.5M H<sub>3</sub>PO<sub>4</sub> is known by the strehlow function Ro(H) or the practical acidity function Ri(H) both equal -1.9 [28,29]. These functions are also named generalized pH in concentrated acid solutions. The addition of H<sub>2</sub>SO<sub>4</sub> shifted to lower values.

The present work aimed to study the temperature effects on welded material corrosion in 5.5M H<sub>3</sub>PO<sub>4</sub> solution in the absence and presence of various concentrations of organic oil of leaves of *Lavandula stoechas* [L] by using potentiodynamic polarization method. Various thermodynamic parameters for inhibitor adsorption on welded steel surface were estimated and discussed. Kinetic parameters for alloy corrosion in absence and presence of the studied inhibitors were evaluated and interpreted.

## EXPERIMENTAL SECTION

### *Conditions and materials*

- 1- The lavender is Moroccan original
- 2 - Ethyl acetate is as the extraction solvent
- 3 - Mounting the soxhlet and hydrodistillation
- 4- Rotary evaporator

### *Extractions technical*

Hydrodistillation (HD)

HD is adapted method for the extraction of an essential oil. The principle of the HD is a distillation heterogeneous.

### *Analytical techniques (CPG-MS)*

The CPG-MS is the coupling GPC analysis which allows to know, in the vast majority of cases, the molecular weight of a compound and to obtain structural information about a molecule from its technical fragmentation.

The tested material was an austenitic stainless steel UB6 alloy, which is classified in the range of high corrosion resistant alloys. This alloy is particularly suitable for applications in the chemical and petrochemical industries. The welding of Alloy UB6 was carried out by the Tungsten Inert Gas (TIG) process. The base material was used as filler too. The chemical composition of the welded alloy is shown in Table 1.

**Table 1: Chemical compositions of the welded metal (WT%)**

| Alloy | Ni | Cr    | Mo   | Cu   | Mn   | Si   | C     |
|-------|----|-------|------|------|------|------|-------|
| UB6   | 26 | 21.50 | 5.20 | 1.20 | 2.50 | 1.45 | 0.025 |

For welding, a tungsten electrode in an argon atmosphere was used. Once the welding was completed, the welded material was cut by the method of water jets cutting the electrode was shaped into cylindrical disk. The exposed area to the solution was 0.6 cm<sup>2</sup> (10 mm in diameter).

In our case, all measurements, electrodes were mechanically polished using successively thinner grade of emery papers (400–4000 grades), and were finally rinsed with distilled water. The tests were carried out in a three-electrode electrochemical cell. The potential of the working electrode was measured against a saturated calomel electrode (SCE) reference electrode. The auxiliary electrode was a platinum (Pt) wire. The electrolyte used in this study was the phosphoric acid (40 wt. %) or 5.5M H<sub>3</sub>PO<sub>4</sub> with the addition of chemical impurities (4 wt. % of H<sub>2</sub>SO<sub>4</sub> and 0.04 wt. % of chloride ions used as KCl). The corrosion behaviour of the alloy was analyzed at different

temperatures (20-80°C). Temperature was controlled by regulating the heater power with a compatible control thermostat.

The experimental apparatus used for electrochemical studies is the PGZ 100 potentiostat, monitored by a PC computer and Voltmaster 4.0 software. Graphs were subsequently scanned anodically at a scan rate of 0.5 mV s<sup>-1</sup>. The potentiodynamic curves of alloy specimens in concentrated phosphoric acid in the absence and in the presence of *Lavandula stoechas* extract were recorded from -0.6V<sub>SCE</sub> to 1.3 mV<sub>SCE</sub>. The tests were repeated at least three times and the scans presented in the paper are one of the obtained curves.

## RESULTS AND DISCUSSION

Following this analysis; the gas chromatography (GC)-mass spectrometry (MS) plant extract showed that the majority compound in the oil extracted is : L-fenchone. (Fig. 1, 2 and 3).

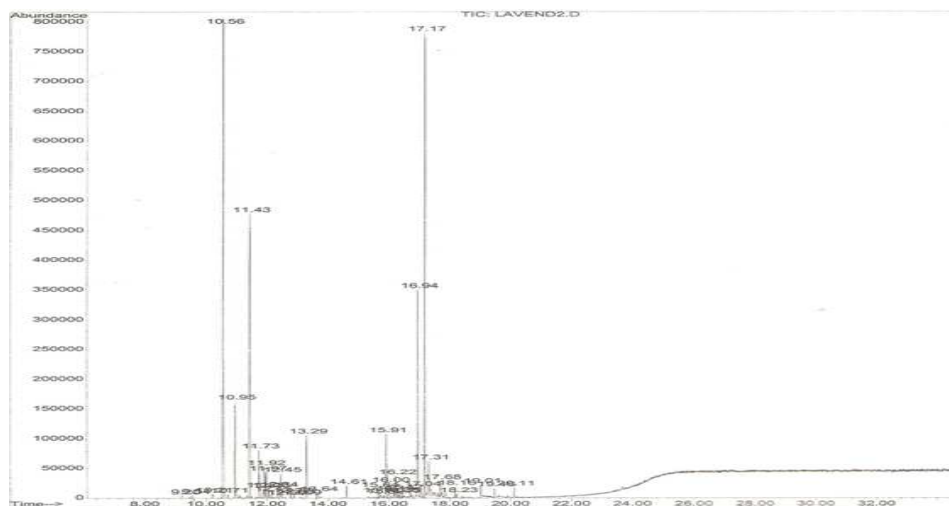


Figure 1 : Spectrum of general plant *Lavandula stoechas*

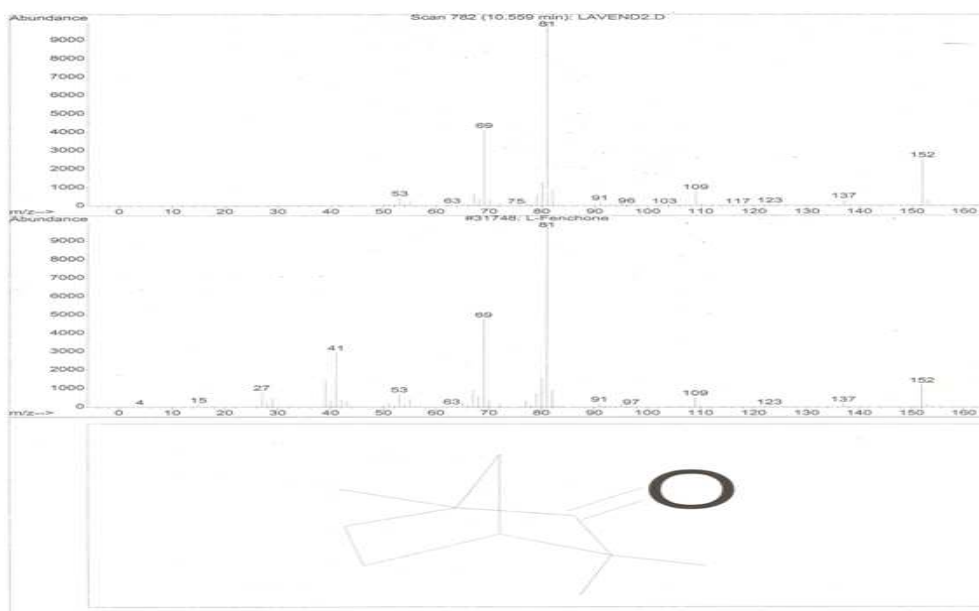


Figure 2: Mass spectrum of the molecule majority with CPG

Essential oils of *Lavandula stoechas* are characterized by the majority compounds as soon as: L-Fenchone: 26.05%. The majoritaire molecule:

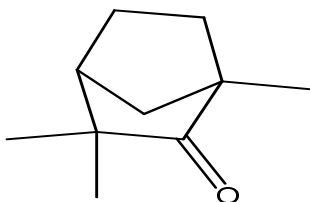


Figure 3: L-Fenchone molecule

#### • Potentiodynamic Polarization Study

The polarization curves of the stainless steel electrode in 5.5M H<sub>3</sub>PO<sub>4</sub>, in the presence and absence of organic oil as would be expected, both cathodic and anodic reactions of stainless steel electrode corrosion were inhibited with the increase of organic oil concentration in acidic solution (Fig. 4). The result suggests that the addition of Oil extracted as inhibitor reduces anodic dissolution and also the hydrogen evolution reaction. For anodic polarization, currents decreased with the time at high over potentials [30].

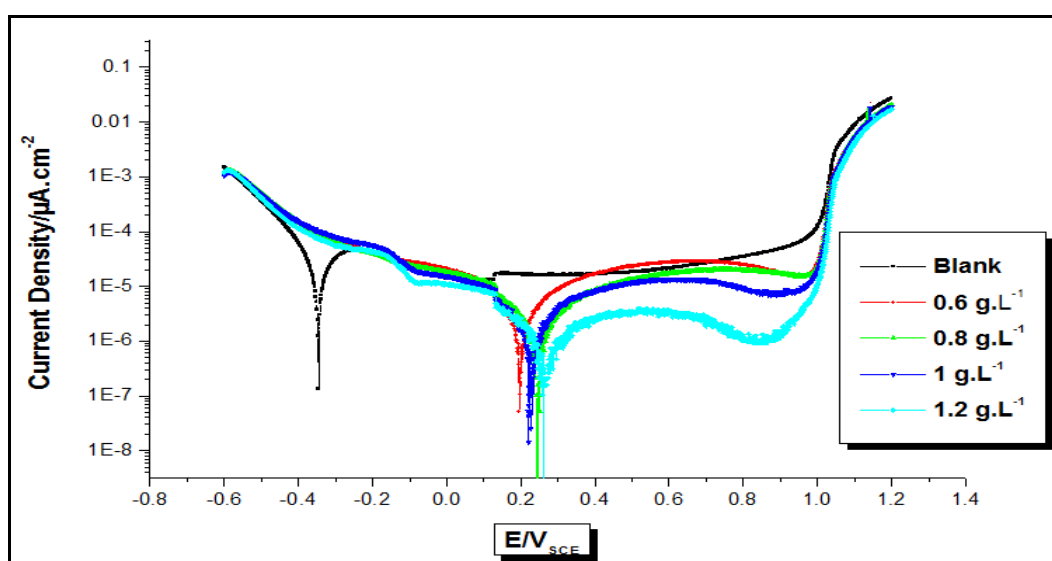


Figure 4. Polarization curves of stainless steel in concentrated H<sub>3</sub>PO<sub>4</sub> at different concentrations of organic oil [L]

We also find that the field of passivity of the welded material is reduced while which increase the concentration of the inhibitor and the corrosion current density is improved.

It can be seen that the electrochemical results show that the welding process shifts corrosion potential  $E_{\text{corr}}$  to more anodic values, the corrosion current and the passivation domain decrease as a consequence of welding, involving a increase in corrosion resistance [31].

Electochemical corrosion Kinetic parameters, corrosion Potential ( $E_{\text{corr}}$ ), cathodic and anodic tafel slopes and corrosion current density ( $I_{\text{corr}}$ ), obtained by extrapolation of the tafel lines, are given in table 2.

The calculated E% of organic oil, in acidic solution is also reported. The inhibition efficiency IE (%) was calculated from polarization measurements according to the relation given below :

$$E = \left(1 - \frac{i_{\text{corr}}}{i_{\text{corr}}^{\circ}}\right) \cdot 100 \quad (1)$$

Where  $i_{\text{corr}}$  and  $i_{\text{corr}}^{\circ}$  are the corrosion current density value with and without inhibitor, respectively, determined by extrapolation of cathodic Tafel lines to the corrosion potential. The  $I_{\text{corr}}$  values decreased considerably in the presence of inhibitor. It can be seen that the cathodic branch recorded in the control medium in the absence and

presence of inhibitor tested exhibit a linear range indicating that the Tafel law holds [32]. The reduction Reaction is carried out under proton pur activation under proton pure activation control. In the anodic branch, the presence of this inhibitor dramatically reduces the anodic current density and shifts the corrosion potential in the positive direction. So this is an anodic inhibitor. They contribute to the formation of a passive barrier layer on the metal surface, which changes the electrochemical reduction by blocking the anodic site. (Headquarters of the oxidation of the metal) [33, 34].

**Table 2: Electrochemical parameters of stainless steel in 5.5M H<sub>3</sub>PO<sub>4</sub> in the presence of different concentrations of [L] at 298 K**

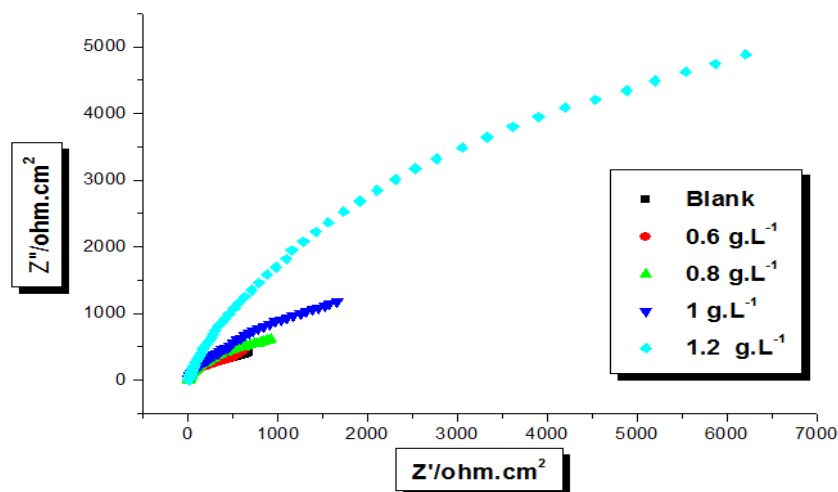
| Alloy                                    | Blank  | 0.6g.L <sup>-1</sup> | 0.8g.L <sup>-1</sup> | 1g.L <sup>-1</sup> | 1.2g.L <sup>-1</sup> |
|--|--------|----------------------|----------------------|--------------------|----------------------|
| I <sub>corr</sub> (uA /cm <sup>2</sup> ) | 47.5   | 14.4                 | 10.4                 | 7.2                | 4.9                  |
| E(mV/SCE)                                | -335   | 119                  | 121                  | 234                | 250                  |
| β <sub>a</sub> (mV)                      | 450.2  | 386.3                | 372.3                | 363.6              | 270.9                |
| β <sub>c</sub> (mV)                      | -303,5 | -445.6               | -400                 | -381               | -322                 |
| % E                                      | -      | 70                   | 78                   | 84.2               | 89                   |

Thus organic oil can be classified as anodic-type inhibitor in 5.5M H<sub>3</sub>PO<sub>4</sub>. E% increased with inhibitor concentration. Maximum inhibition efficiency was obtained at a concentration of 1.2g.L<sup>-1</sup>.

#### • *Electrochemical impedance spectroscopy measurements*

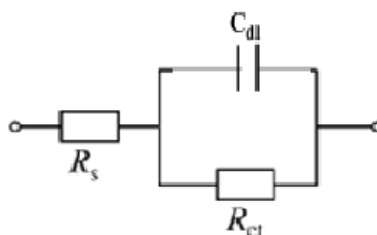
The corrosion behaviour of welded material in 5.5M phosphoric acid solution in the presence and absence of Organic oil, is also investigated by the electrochemical impedance spectroscopy (EIS). The measurements were performed at 293 K in the corrosive environment. Fig. 5 shows the corresponding Nyquist diagram. The impedance parameters derived from these investigations are mentioned in Table 3.

From Fig. 5, the obtained impedance diagrams (almost a semi-circular appearance), indicates that a charge transfer process mainly controls the corrosion of welded material [35]. The general shape of the curves is very similar for all samples; the shape is maintained throughout the whole concentration, indicating that almost no change in the corrosion mechanism occurred due to the inhibitor addition [36]. The R<sub>t</sub> values increased with the increase of the concentration of organic oil. The values of double layer capacitance are also brought down to the maximum extent in the presence of inhibitor and the decrease in the values of C<sub>dl</sub> follows the order similar to that obtained for I<sub>corr</sub> in this study.



**Figure5. Nyquist diagrams for welded material in 5.5M H<sub>3</sub>PO<sub>4</sub> containing different concentrations of organic oil [L]**

to account for the corrosion behavior of the stainless steel in concentrated phosphoric acidic solution with the presence of the inhibitor and to simulate the metal/acidic solution interface, an equivalent circuit model consists of solution resistance (R<sub>s</sub>), double layer capacitance (C<sub>dl</sub>), charge transfer resistance (R<sub>ct</sub>) has been shown in Fig.5 in which the C<sub>dl</sub> and R<sub>ct</sub> are parallel to each other.

Figure 6. Equivalent circuit model for the corrosion for welded material in 5.5M H<sub>3</sub>PO<sub>4</sub> at 298 KTable 3. Impedance parameters and inhibition efficiency for the corrosion of welded material in 5.5M H<sub>3</sub>PO<sub>4</sub> at various concentrations of [L] at 298 K

| Alloy                                  | Blank | 0.6g .L <sup>-1</sup> | 0.8 g .L <sup>-1</sup> | 1 g .L <sup>-1</sup> | 1.2 g .L <sup>-1</sup> |
|--|-------|-----------------------|------------------------|----------------------|------------------------|
| R <sub>T</sub> (Ω cm <sup>2</sup> )    | 129   | 324                   | 474                    | 480                  | 620                    |
| C <sub>dl</sub> (μF cm <sup>-2</sup> ) | 140   | 102.4                 | 118.7                  | 42.3                 | 50.9                   |
| % E                                    | -     | 60                    | 72.7                   | 73.1                 | 79.1                   |

The parameters deduced are grouped in Table 3. Charge-transfer resistance values (R<sub>T</sub>) and double layer capacitance values (C<sub>dl</sub>) have been obtained from impedance measurements as described previously. The following relation is used to calculate E (%):

$$E\% = \left(1 - \frac{R_T^*}{R_T}\right) \cdot 100 \quad (2)$$

Where R<sub>T</sub> and R<sub>T</sub><sup>\*</sup> are the charge-transfer resistance values with and without inhibitor, respectively.

Examination of Table 3 reveals that, more and more the organic oil [L] concentration increases, R<sub>T</sub> rises to higher values showing that [L] inhibit corrosion reaction. The decrease of C<sub>dl</sub> is interpreted by the adsorption of inhibitor molecules on the metal surface [37- 38]. The results obtained from the polarization technique in acidic solution were in good agreement with those obtained from the electrochemical impedance spectroscopy (EIS).

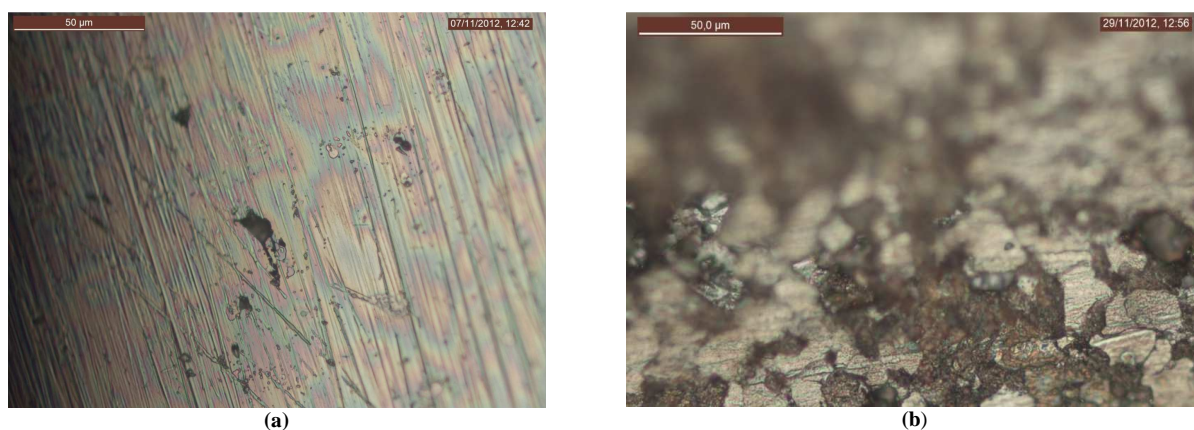


Figure 7 : Examination by electron microscopy of the surface of the alloy welded phosphoric medium  
(a): 5.5M H<sub>3</sub>PO<sub>4</sub> without addition of inhibitor ;(b): 5.5M H<sub>3</sub>PO<sub>4</sub> + 1.2g.L<sup>-1</sup> organic oil[L]

#### • Effect of temperature

##### *Adsorption isotherm*

In the acid environments, the inhibitors act at first by adsorption on the surface of metals before intervening in the reaction processes of corrosion to decrease the speed. The phenomenon of adsorption is made according to equation (3):



When the equilibrium of the process described in equation (3) is reached, it is possible to obtain different expressions of the adsorption isotherm plots. The degree of surface coverage  $\theta$  can be plotted as a function of the concentration of the inhibitor under test [39] in 5.5M  $\text{H}_3\text{PO}_4$ . Langmuir mathematical expressions are given as follow (4):

$$\frac{C_{inh}}{\theta} = \frac{1}{K_{ads}} + C_{inh} \quad \text{With} \quad K_{ads} = \frac{1}{C_{\text{H}_2\text{O}}} \exp\left(-\frac{\Delta G_{ads}^\circ}{RT}\right) \quad (4)$$

Where  $C_{inh}$  is the concentration of the inhibitor,  $K_{ads}$  is the adsorptive equilibrium constant;  $\theta$  is the surface coverage and the standard adsorption free energy  $\Delta G_{ads}^\circ$ . The relationship between  $\frac{C_{inh}}{\theta}$  and  $C_{inh}$  presents linear behaviour at the temperature with slope equal to unity. For this reason Langmuir adsorption isotherm was preferred to fit the results. A plot of  $C/\theta$  versus  $C$  (Fig. 8) gives a straight line with an average correlation coefficient of 0.99867 and a slope of nearly unity (1.07) suggests that the adsorption of [L] can be expressed by the following equation 5:

$$\Delta G_{ads}^\circ = -RT \ln (C_{\text{H}_2\text{O}} \cdot K_{ads}) \quad (5)$$

In equation (5), we use  $C_{\text{H}_2\text{O}}$  in g/L ( $10^3$ g/L) and  $K_{ads}$  in L/g, the unity of  $\Delta G_{ads}^\circ$  depends only on the factor  $RT$  ( $\text{kJ}\cdot\text{mol}^{-1}$ ).

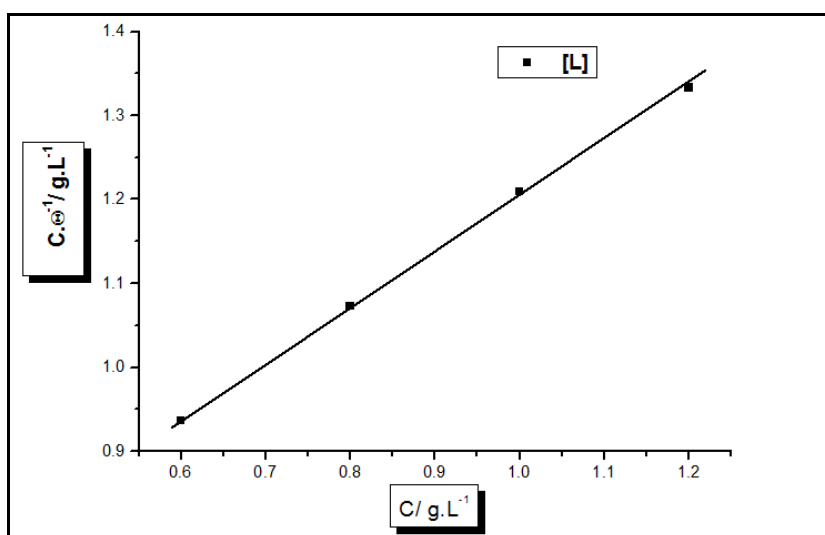


Figure 8: Langmuir isotherm adsorption model on the stainless steel surface of [L] in 5.5 M  $\text{H}_3\text{PO}_4$

However, the use of an extract which contains an infinity of compounds do not promote the calculation of the free enthalpy of adsorption as already demonstrated in several papers [40,41].

#### ***Kinetic-thermodynamic corrosion parameters***

As noticed previously, the adsorption process was well elucidated by using a thermodynamic model. In addition, a kinetic-thermodynamic model was another tool to explain the mechanism of corrosion inhibition for an inhibitor. We were interested in exploring the activation energy of the corrosion process and the thermodynamics of adsorption of organic oil; this was accomplished by investigating the temperature dependence of the corrosion current obtained using extrapolation method.

The corrosion current density decreased with one order of magnitude with increasing temperature, both in uninhibited and inhibited solutions (table 4).

**Table 4: The influence of temperature on the electrochemical parameters for stainless steel electrode immersed in 5.5 M H<sub>3</sub>PO<sub>4</sub> and in 5.5 M H<sub>3</sub>PO<sub>4</sub> + 1.2g.L<sup>-1</sup> [L]**

|        | 5.5M H <sub>3</sub> PO <sub>4</sub> |  | 1.2g.L <sup>-1</sup> +5.5M H <sub>3</sub> PO <sub>4</sub> |  | %E |
|--------|-------------------------------------|--|---|--|----|
|        | E <sub>corr</sub> (mV/SCE)          | I <sub>corr</sub> (μA /cm <sup>2</sup> ) | E <sub>corr</sub> (mV/SCE)                                | I <sub>corr</sub> (μA /cm <sup>2</sup> ) |    |
| 293 °K | -335                                | 47.5                                     | 149   | 4.9                                      | 90 |
| 313 °K | -226                                | 50.0                                     | 112   | 10.8                                     | 82 |
| 333 °K | 149                                 | 61.8                                     | 125   | 20                                       | 75 |
| 353 °K | 156                                 | 79.7                                     | 133.7   | 32.1                                     | 60 |

The corrosion current density for welded stainless steel increased more rapidly with temperature in the absence of inhibitor (Blank).

The welded material presented and shows a more active behavior and sensitivity to corrosion and temperature, it was found that increasing the temperature even in the presence of the inhibitor decreases its effectiveness [11]. The corrosion reaction can be regarded as an Arrhenius-type process; the rate is given by :

$$I_{corr} = K \cdot \exp\left(\frac{E_a}{RT}\right) \quad (6)$$

Where k is the Arrhenius pre-exponential constant, and E<sub>a</sub> is the activation corrosion energy for the corrosion process.

The Arrhenius plots present of the logarithm of the corrosion current density reciprocal of temperature for 5.5 M H<sub>3</sub>PO<sub>4</sub>, without and with addition of [L] (fig.8). The E<sub>a</sub> values were determined from the slopes of these plots and are calculated to be E<sub>a</sub> = 10.13 kJ/mol and 35 kJ/mol While the higher value of the activation energy of the process in an inhibitor's presence when compared to that in its absence is attributed to its physical adsorption [42,43], its chemisorptions is pronounced in the opposite case [44,45]. The higher value of E<sub>a</sub> in the presence of [L] compared to that in its absence and the decrease of its E% with temperature increase can be interpreted as an indication of physical adsorption.

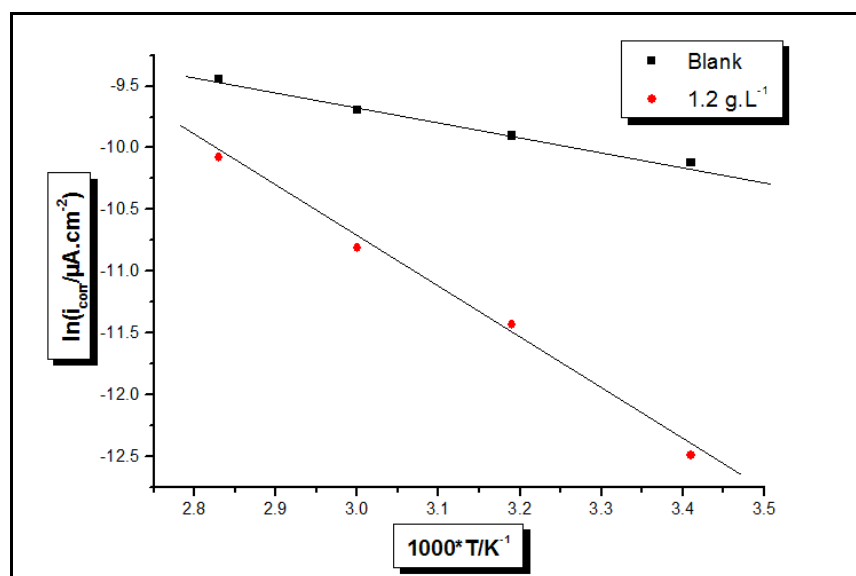


**Figure 9: Arrhenius straight lines calculated from corrosion rate of stainless steel in 5.5M H<sub>3</sub>PO<sub>4</sub> and 5.5M H<sub>3</sub>PO<sub>4</sub> + 1.2g.L<sup>-1</sup> [L]**

## CONCLUSION

Electrochemical study showed that plant extract is a good corrosion inhibitor and acts as an anodic-type inhibitor in concentric phosphoric acid. The inhibition efficiency increases with increasing inhibitor concentrations to attain a maximum value of 89% for inhibitor [L] at 1.2 g.L<sup>-1</sup>. The inhibition efficiency of [L] decreases slightly with the temperature and the addition of [L] leads to increase of corrosion activation energy.

The adsorption of [L] on the stainless steel surface in phosphoric acid obeys the Langmuir adsorption isotherm model.

Finally we can deduce that *Lavandula stoechas* oil can play an important role in the fight against corrosion.

#### REFERENCES

- [1] H Zarrok; A Zarrouk; B Hammouti; R Salghi; C Jama; F Bentiss; *Corros Sci*, (2012), 64, 243
- [2] N Bui; A Irzho; F Dabosi; A Guenbour; A Ben Bachir; *Ann Chim* (1983), 8, 411
- [3] A Guenbour; J Faucheu; A Ben Bachir; N Bui; F Dabosi; *Brit Corros J*, (1988), 23(4), 234
- [4] A Guenbour; J Faucheu; A Ben Bachir; *Corrosion*, (1988), 44 214
- [5] A Guenbour; N Bui; J Faucheu; Y Segui; A Ben Bachir ; *Corros Sci*, (1990), 30, 189
- [6] A Bellaouchou; A Guenbour; A Ben Bachir ; *JM Costa; Corros Sci*, (1993), 63, 656
- [7] A Ousslim; A Aouniti; K Bekkouch; A Elidriissi, B Hammouti, *Surface Review and Letters*; (2009), 16, 609
- [8] N Nassif ; *Surf Technol*, (1985), 26, 189
- [9] P Marcus; J Oudar ; *Appl Surf Sci*, (1982), 3, 29
- [10] P Becker; Phosphates and Phosphoric Acid Raw Materials, Technology and Economics of the Wet Process, second ed, M Dekker, New York, (1989)
- [11] H Iken; R Basseguy; A Guenbour; A Ben Bachir; *Electrochim Acta*, (2007), 52, 2580
- [12] A Guenbour; MA Hajji; EM Jallouli; A Ben Bachir; *Appl Surf Sci* , (2006), 253, 2362
- [13] S Bakour; A Guenbour; A Bellaouchou; C Escrivà-Cerdán; R Sánchez-Tovar; R Leiva- García; García-Antón ; *J Int J Electrochem Sci*, (2012), 7, 10530-
- [14] M Ibáñez-Ferrándiz; E Blasco-Tamarit; D Miguel García-García; J Garcia-Anton; A Guenbour ; *ECS Trans*, (2010), 25, 49-61
- [15] I El Ouali; B Hammouti; A Aouniti; Y Ramli; M Azougagh; EM Essasi; M Bouachrine; *J Mater Environ Sci*, (2010), 1, 1
- [16] SS Abd El Rehim; MAM Ibrahim; KF Khaled; *J Appl Electrochem*, (1999), 29, 593
- [17] B Mernari; H El attari; M Traisnel; F Bentiss; M Lagrenee; *Corros Sci*, (1998), 40, 391
- [18] F Bentiss; M Lagrenee; M Traisnel; B Mernari; H El attari; *J Appl Electrochem*, (1998), 29, 1073
- [19] B Mernari; L El Kadi; S Kertit; *Bull Electrochem*, (2001), 17, 115
- [20] M Bouklah; N Benchat; A Aouniti; B Hammouti; M Benkaddour; M Lagrenée; H Vezin; F Bentiss; *Progress in Organique Coating*; (2004), 51, 118
- [21] F Bentiss; C Jama; B Mernari; H El Attari; L El Kadi; M Lebrini; M Traisnel; M Lagrenée; *Corros Sc*, (2009), 51, 1628
- [22] M Bouklah; B Hammouti; M Lagrenée; F Bentis ; *Corros Sci*, (2006), 48, 2831
- [23] MA Quraishi; A Singh; VK Singh; K Yadov; AK Singh; *Mater Chem Phys*, (2010), 122, 114
- [24] SA Umoren; IB Obot; EE Ebenzo; NO Obi-Egbedi; *Int J Electrochem Sci*, (2008), 3 1029
- [25] M Boudalia; A Guenbour; A Bellaouchou; A Laqhaili; M Mousaddak; A Hakiki; B Hammouti; E.E. Ebenso, *Int J Electrochem Sci*, (2013), 8, 7414
- [26] H Bouammali; A Ousslim; K Bekkouch; B Bouammali; A Aouniti; SS Al-Deyab; C Jama; F Bentiss; B Hammouti; *Int. J. Electrochem. Sci.*, (2013), 8, 6005
- [27] B Zerga; M Sfaira; Z Rais; M Ebn Touhami; M Taleb; B Hammouti; B Imelouane ; A Elbachir; *Materiaux et Technique*, (2009), 97, 297
- [28] B Hammouti; H Oudda; A Benayada; A El Maslout; J Bessière; *Ber Bunsenges Phys chem*, (1997), 101, 65
- [29] B Hammouti ; H Oudda ; A El Maslout; A Benayada; *Trans SAEST*, (2004), 39, 81
- [30] A Ghazoui; R Saddik, N Benchat; B Hammouti; M Guenbour; A Zarrouk; M Ramdani *Der Pharma Chemica*, (2012), 4, 352
- [31] M Lagrenée; B Mernari; M Bouanis; M Traisnel; F Bentiss; *Corros Sci*, (2002), 44, 573
- [32] A Ghazoui; R Saddik; B Hammouti; A Zarrouk; N Benchat; A Guenbour; SS Al-Deyab; I Warad; *Int J Electrochem Sci*, (2012), 7, 7080
- [33] AV Benedetti; PTA Sumodjo; K Nobe; PL Cabot; WG Proud; *Electrochim Acta*, (1995), 40, 2657
- [34] C Guo-hao; Jing-Mao; *Z Chem Res Chinese Univ*, (2012), 28, 691
- [35] R Rosliza; Wan Nik ,WB; Senin; HB *Mater Chem Phys*, (2008), 107, 281
- [36] EE Oguzie; Onuchukwu ; *AI Corros Rev*, (2007), 25, 355
- [37] F Bentiss; M Lagrenee, M Traisnel, JC Mand Hornez.; *Corros Sci*, (1999), 41, 789
- [38] E Mccarfferty; N hackerman; *J Electrochem Soc*, (1972), 119, 146
- [39] I Langmuir; *Amer, J Chem Soc*, (1947), 39, 1848
- [40] M Belkhaouda; L Bammou; R Salghi; A Zarrouk; H Zarrok; M Assouag; Al- S S Deyab; B Hammouti; *Der Pharmacia Lettre*, (2013), 5 (3), 297

- [41] D Ben Hmamou; R Salghi; A Zarrouk; H Zarrok; O Benali; M Errami; B Hammouti; *Res. Chem. Intermed.*, (2013), 39, 3291
- [42] H Zarrok; A Zarrouk; B Hammouti; R Salghi; C Jama; F Bentiss; *Corros Sci*, (2012), 64, 243
- [43] AP Yadav; A Nishikata; T Tsum; *Corros. Sci.* (2004), 46, 169
- [44] M Benabdellah; A Tounsi; KF Khaled; B Hammouti; *Arab J Chem*, (2011), 4, 17
- [45] S Sankarappavinasam; F Pushpanaden; M Ahmed; *Corros. Sci.* (1991), 32, 235